

ac Susceptibility in Granular Superconductors: Theory and Experiment.

A. Kunold, M. Hernández, A. Myszkowski, J.L. Cardoso, P. Pereyra
Departamento de Ciencias Básicas, UAM/Azcapotzalco, Av. S. Pablo 180,
México D.F. 02200

(November 4, 2018)

Abstract

A phenomenological theory to describe the electromagnetic properties of granular superconductors, based on known bulk superconductors expressions and conventional Josephson's junctions tunneling currents, is presented and successfully used to fit distinct experimental results for the magnetic susceptibility χ as a function of the temperature and the applied magnetic field of rather different samples.

I. INTRODUCTION

The influence of the granular structure on the electromagnetic superconducting properties has been consistently recognized [1], and simple formulas and models were used to account for the main features of the ac susceptibility $\chi(B, T)$ as a function of temperature (T) and magnetic field (B). The critical state model [2], and its extended versions [1,3], have been useful in interpreting the observed values of the magnetic response of type-II superconductors and the underlying interplay between pinning and creep forces on Josephson vortices in the grain and intergrain regions, both in zero-field cooling and field cooling experiments [5–10]. Other effects, such as phase coherence and decoherence phenomena, peculiar to Josephson junctions and the quantum interference effects in the loops, add extra complexity

to the polycrystalline magnetic response. In general, these effects have been neglected or taken into account only partially (or indirectly) to describe the ac susceptibility in polycrystalline superconductors. It is the purpose of this paper to consider them explicitly, to deduce a simple formula to describe the granular superconductors susceptibility in terms of the Josephson junction and loop areas, the penetration depth, the decoherence decay length and a critical exponent, and to show the ability of the formula to account qualitatively and quantitatively the rather complex behavior of $\chi(B, T)$. To illustrate this, magnetic response data of quite different samples are considered and fitted with fairly good results.

The understanding of the granular structure influence on the electromagnetic properties is not only of relevant interest but also of a challenging nature. Many effects, related with the phase coherence and Josephson vortices pinning and displacements, combine to give rise to flourishly different experimental results. Careful measurements reveal subtle and systematic quantum coherence phenomena that affect the order parameter of adjacent superconducting grains and produce well defined field- and sample-dependent oscillations, apparent in the critical transport and screening currents behavior [11–17].

In the last years we have been interested in high precision measurements of critical transport and screening currents as functions of the temperature, magnetic field and the granularity of the superconducting samples. The main idea in these experiments was to reduce the effects of macroscopic averaging [18–20]. Recently, a phenomenological theory of the Josephson junction between two superconducting grains, taking into account the effects of coherence and decoherence decay lengths on the order parameter, has been suggested to describe the Ambegaokar-Baratoff to Ginsburg-Landau transition in the temperature behavior of the critical transport current [21].

In the present paper, we study the behavior of the magnetic susceptibility χ as a function of the temperature and the external magnetic field. The measurement of χ permits to study the tunneling phenomena far away from the critical points and limits the current paths to a few adjacent grains. For this report we consider two quite different samples: a "bad" and porous sample B, with irregular grains and low magnetic susceptibility, and a "good" sample

G, with closely packed parallelepiped shaped grains and much higher value of χ (see Figure 1). The "bad" sample susceptibility also presents oscillations and a pronounced decrease of χ with increasing magnetic field (see Figure 2).

The contents of this paper are as follows. In the second Section we recast the Clem's picture of the screening currents in granular systems. We then recall, in Section III, some basic and known expressions of the superconducting theory and 'put them together' in a kind of phenomenological formula to describe the real part of the ac susceptibility. In Section IV, this phenomenological theory is applied to rather different granular superconductors, and finally in Section V we give a brief discussion.

II. SCREENING CURRENTS IN GRANULAR SYSTEMS

It is well known that the basic magnetic properties of ceramics are created by the currents circulating inside the grains, which tend to expel the external magnetic field from parts of the volume (regions of the type I in Figure 3) and thus lead to a diamagnetic behavior. Following Clem's picture of the granular behavior, we distinguish three characteristic regions as shown in Figure 3. In this Figure, the screening current in regions II, responsible for the basic diamagnetic properties of the material, is distributed as suggested in the lower part of the Figure. The current density reaches its maximum (critical value) at the boundary of this region II, and beyond this region's "surface", i.e. in region III, there is no screening current.

Josephson tunneling junctions are formed in regions III and IV and the Josephson tunneling process connects the 'surfaces' of regions II in adjacent grains, which are of course in a critical state. It is important to stress that, even if the applied magnetic field is weak, far away from its critical value (from the macroscopic point of view), the screening currents and the local magnetic field on each grain determine a local criticality and the penetration length, the existence or non existence of screening currents and, consequently, the position of the surfaces limiting the regions II, which (from the microscopical point of view) are in critical condition.

The ceramic structure permits the flowing of circulating currents over clusters of grains. The represented cluster of three grains (in Figure 4) is only an example; there is a possibility of current paths over a great amount of grains with Josephson type junctions between each pair. The corresponding currents produce some additional magnetic effects and modify the magnitude of χ . These currents are, of course, regulated by the quantum interference phenomena and the Josephson junctions.

In Figure 4, the current 1 flowing over the external part of a cluster circulates in the same direction as the intragranular currents. This current has a diamagnetic character and raises the value of $|\chi|$. However, it does not expel the external magnetic field completely from the junctions. The internal part of the circuit contains the current 2, flowing in the opposite direction, though alongwith the currents inside the grains, it is of paramagnetic character [14,22,23], and permits the passage of some vortices of external magnetic field through the intergranular region V.

III. THEORY OF THE MAGNETIC RESPONSE IN POLYCRYSTALLINE SAMPLES

As in the case of the critical transport current, the behavior of the magnetization current presents systematic sample-dependent oscillations. These oscillations in polycrystalline and highly random systems, with low density of irregular grains, can also be explained reasonably well in terms of the superposition of Josephson junction and quantum-interfering intergrain currents. Therefore, the total current contains the contributions of the Josephson type currents

$$j_J = j_c \frac{\sin(\pi\phi_J/\phi_o)}{\pi\phi_u/\phi_o} \quad (1)$$

and loop currents

$$j_l = j_J \cos(\pi\phi_l/\phi_o). \quad (2)$$

Here j_c is the lowest junction's critical current in the loop l , ϕ_J is the magnetic flux through the junction's area given by

$$\phi_J = BS_J = B(2\lambda_J + d)(r_J - 2\lambda_J), \quad (3)$$

and ϕ_l the magnetic flux through the loops's area taken as

$$\phi_l = BS_l = B\pi(r_l + \lambda_J)^2. \quad (4)$$

At this level we have the fundamental quantities in terms of the basic granular parameters: the distance between two adjacent grains d , the junction size r_J , the loop area r_l and the magnetic penetration length λ_J whose temperature dependence is

$$\lambda_J = \lambda_o(1 - T/T_c)^{-\beta}, \quad (5)$$

with λ_o the zero temperature penetration depth and β a positive critical exponent (in BCS theory $\beta = 1/2$).

In macroscopic samples, different areas of junctions and loops are possible. Therefore, the total magnetization current j_M can be thought of as the superposition of a collection of loop currents j_l modulated by j_J . Thus, to describe the magnetization current we shall consider the expression

$$j_M = \sum_{l,J} j_c(T, B) \left| \frac{\sin(\pi\phi_J/\phi_o)}{\pi\phi_J/\phi_o} \right| \cos(\pi\phi_l/\phi_o) \quad (6)$$

where

$$j_c(T, B) = j_o(1 - T/T_c)^\alpha \exp \left[-\frac{2\lambda_o}{\zeta_o}(1 - T/T_c)^{\alpha-0.5} + \frac{2\lambda_o}{\zeta_o} \right] \quad (7)$$

and ζ_o is the zero temperature decoherence length defined as in reference [21]. In polycrystalline samples many of these parameters vary randomly. Notice that the temperature dependence is not completely factorized because both ϕ_J and ϕ_l depend also on the temperature, and α and ζ_o depend on the magnetic field.

On the other hand, taking into account that the magnetization current and the susceptibility are quantities proportional to each other, it is possible to conclude that the real part of the susceptibility χ is described by a similar function [4], i.e.

$$\text{Re } \chi_c(T, B) = \chi_c(0, B) (1 - T/T_c)^\alpha \exp \left[-\frac{2\lambda_o}{\zeta} (1 - T/T_c)^{\alpha-0.5} + \frac{2\lambda_o}{\zeta} \right] \quad (8)$$

The magnetic field dependence is like that in equation (7). For small values of B , applied in the experimental measurements discussed below, we can safely assume that the sum upon the junction and loop indices can be substituted by a contribution of a junction and a loop with "effective" areas $S_{J,eff}$ and $S_{l,eff}$, such that

$$\chi_c(0, B) = \chi_c(0, 0) \left| \frac{\sin(\pi B S_{J,eff}/\phi_o)}{(\pi B S_{J,eff}/\phi_o)} \right| \cos(\pi B S_{l,eff}/\phi_o) \quad (9)$$

These equations will be used, in the next section, to adjust the experimental points choosing different values for the parameters α , ζ , χ_o , $S_{J,eff}$ and $S_{l,eff}$. Taking $d \approx 0$, and the "average" value of λ_o ($\lambda_o \approx 3000nm$) [24], it is also possible to estimate the "effective" values of $r_{J,eff}$ and $r_{l,eff}$.

IV. EXPERIMENTAL RESULTS AND DISCUSSION

As mentioned above, a more flexible but rigorous application of the definition of the critical parameter lead us, as in previous works, to determine reliable and precise measurements of critical transport currents as functions of the magnetic field, based on direct transport critical currents measurements for different temperatures, [18–20]. Similarly, direct temperature dependence of the magnetic susceptibility χ in polycrystalline superconducting samples allows us to determine, with high precision, the magnetic field dependence of χ for different fixed temperatures.

In the experimental procedure, partially explained in references [18–20], the temperature is slowly raised by natural heating during the experiment, while the external magnetic field is kept constant. In this way, a set of temperature dependent susceptibility data is obtained.

Changing the magnetic field, a new set of data $\chi = \chi_B(T)$, with B taken as a parameter, is obtained. All these data $\chi_B(T)$, corresponding to different applied magnetic fields, generate a surface in the B - T - χ space and define the susceptibility $\chi = \chi(B, T)$.

A series of Y -based samples were prepared by standard solid state reactions. The mixture of high purity Y_2O_3 , Ba_2CO_3 and CuO powders were ground, pelleted at a pressure of $5\text{tons}/\text{in}^2$ and pre-fired at 910°C for 24 hours. This procedure was repeated three times for heating temperatures of 920°C , 930°C and 940°C . An extra sintering of compact pellets in oxygen flow at 950°C for 24h was followed by a slow cooling in oxygen flow. The cooling rate of this stage was varied in order to get two samples with different grain sizes. In Figure 1 we observe the different structures of samples G and B that will be analyzed in this paper – sample B with grains separated by inter granular dark regions and sample G, with closely packed grains and a minimum spacing between them (see Figure 1).

The samples were cut and polished in the shape of thin disks and then mounted on cooper paste in order to decrease the temperature gradient. The temperature of the sample was measured with a platinum resistor and a Lake Shore detector. These samples were cooled in an APD SCS cryostat adapted for AC susceptibility measurements. The output signal was processed with a Lock-in amplifier.

In Figure 2, the susceptibilities of samples G and B, are plotted together to make evident the influence of the physical structure on the behavior of χ as a function of the temperature and the external magnetic field. In the case of sample B, χ takes relatively low values even for a low temperature (35K) and zero magnetic field (see Figure 5), and the constant temperature susceptibility as a function of the magnetic field decreases with visible oscillations due to the Josephson junction effects. The susceptibility reduces rapidly with increasing temperature, from 0.49 (at $T = 35\text{K}$) to 0.38 (at $T = 70\text{K}$). At $B \approx 250\mu\text{T}$, the magnetic field effect on χ is weaker because some junctions are already disconnected and χ is controlled mainly by the diamagnetic properties of the grains. The high-temperature curve oscillates with the magnetic field less than the low temperature curve for the same reason.

The susceptibility shown in Figure 6 for sample G exhibits a completely different behavior

and higher values (≈ 0.73 for $T = 35K$ and $B \approx 50\mu T$). It is obvious that the intergrain currents can flow easier through short junctions, and thus screen the external magnetic field more efficiently. The susceptibility decreases with the magnetic field, but without visible oscillations. The reduced width of the Josephson junctions does not permit an appreciable penetration of the magnetic field into them. The decrease of χ with temperature corresponds to an increase of the type III regions, where vortices of the external magnetic field can penetrate.

TABLES

TABLE I. Parameters used to fit data, in figures 5 and 6 and some estimated geometrical parameters. We give here the critical temperature T_c , the effective grain and loop areas $S_{J,eff}$ and $S_{l,eff}$, the critical exponent α , the decoherence length ζ_o at $T = 0$, and the susceptibility χ_o at $B = 0$. We give also the estimated values of the Josephson junction and loop effective radius $r_{J,eff}$, $r_{l,eff}$, for samples B and G.

Sample	B	G
T_c [K]	91.0	91.0
$S_{J,eff}$ [μm^2]	0.708	0.834
$S_{l,eff}$ [μm^2]	507.75	-- -- [†]
$r_{J,eff}$ [μm]	1.78	1.99
$r_{l,eff}$ [μm]	12.713	-- -- [†]
ζ_o [nm]	41 – 255	35 – 211
α	0.52 – 0.98	0.53 – 0.83
$\chi_c(0,0)$	0.4819	0.7273

[†] Within the fitting resolution negligible loop contribution is found.

In all cases, it was possible to fit the data by choosing the values of r_J , r_l , ζ , α and $\chi_c(0, 0)$, as indicated in Table I. Besides the sample-dependent (zero field and zero temperature) scaling susceptibility factor $\chi_c(0, 0)$, which comprises the global magnetic field response, the critical exponent α , the decoherence length ζ , and the Josephson junction and loop effective areas values, correspond quite well to the samples characteristics. In the case of sample B (see Figure 5) the adjustment is not exact, due to the irregular shapes of the grains and junctions. The fitting is far more better for sample G, where the loops of currents do not play an important role (see Figure 6). The major difference within the parameter values in Table I appears in the parameter r_l , which for sample G is practically vanishing, while for sample B it has a relatively high value. In sample B the porous structure forces the Cooper pairs to larger loops around the intergrain regions V. On the contrary, in sample B such loops are not necessary because the grains are arranged very closely.

Concerning the critical exponent α appearing in the polynomial and exponential temperature dependent factors, we notice that their values remain between 1/2 and 1 (increasing with the magnetic field), as was found already in previous reports, where the order parameter was shown to decay exponentially because of the intergrain tunneling process. Finally, the fitting values of the decoherence length ζ , are more or less the same for both samples and, as expected, grow with the magnetic field.

V. CONCLUSIONS

In this paper we studied another physical quantity characterizing the polycrystalline superconductors electromagnetic properties. We show that, as for the critical transport currents, the Josephson and loop's interfering currents have, depending on the sample quality, different degrees of influence on the magnetic field response. The susceptibility of equations (8) and (9) gives reasonably good predictions on its behavior as a function of the temperature and the external magnetic field. The oscillations of χ , observed experimentally, are well explained on the basis of the quantum interference theory, the exponential suppression

of the order parameter induced by tunneling processes, and the polynomial temperature dependence known from the standard theory.

ACKNOWLEDGMENTS

We acknowledge discussions with Professor H. Simanjuntak and the partial support of CONACyT of México under Project No. 350-E9301 and of The Abdus Salam International Center for Theoretical Physics, Trieste-Italy.

REFERENCES

- [1] J. R. Clem, H. R. Kerchner, and S. T. Sekula, Phys. Rev. B, 14, 1893 (1976), J. R. Clem, z. Hao, Phys. Rev. B, 48, 13774 (1993).
- [2] Phys. Rev. Lett. 8, 250 (1962), Rev. Mod. Phys. 36, 31 (1964)
- [3] Y. Kimishima, K. Kamimura, Y. Ichiyanagi, Physica C, 329, 17 (2000).
- [4] John R. Clem, Physica C 153-155, 50 (1988).
- [5] S. D. Murphy, K. Renouard, R. Crittenden and s. M. Bhagat, Sol. Stat. Com. 69, 367 (1989).
- [6] V. G. Kogan, M. M. Fang and S. Mitra, Phys. Rev. B, 38, 11958 (1988)
- [7] J. F. Beadoin, F. Weiss, J. P. Senateur, T. Verhaege, P. Dubots, Physica C, 153-155, 1397 (1988).
- [8] E. Bruneel, A. J. Ramirez-Cuesta, I. Van Driessche and S. Hoste, Phys. Rev. B, 61 9176 (2000).
- [9] S. Ravi, Physica C, 330, 58 (2000).
- [10] O. F. de Lima and C. A. Cardoso, Phys. Rev. B 61, 11722 (2000).
- [11] John R. Clem and A. Sánchez, Phys. Rev. B. **50**, 9355 (1994). Lett. **74**, 1202 (1995).
- [12] Y. Dagan, R. Krupke and G. Deutscher, Phys. Rev. B **62** (2000) 146.
- [13] F. Holtzberg, Phys. Rev. B **49** (1994) 4384.
- [14] P. Barbara, F.M. Aranjú-Moreira, A.B. Cawthorne and C.J. Lobb, Phys. Rev. B **60**, (1999) 7480.
- [15] R.G. Mints, Sov. Phys. Solid State **30** (11) 1988.
- [16] J.L. González, P. Muné, L.E. Flores, E. Altshuler, Physica C **255** (1995) 76-80.

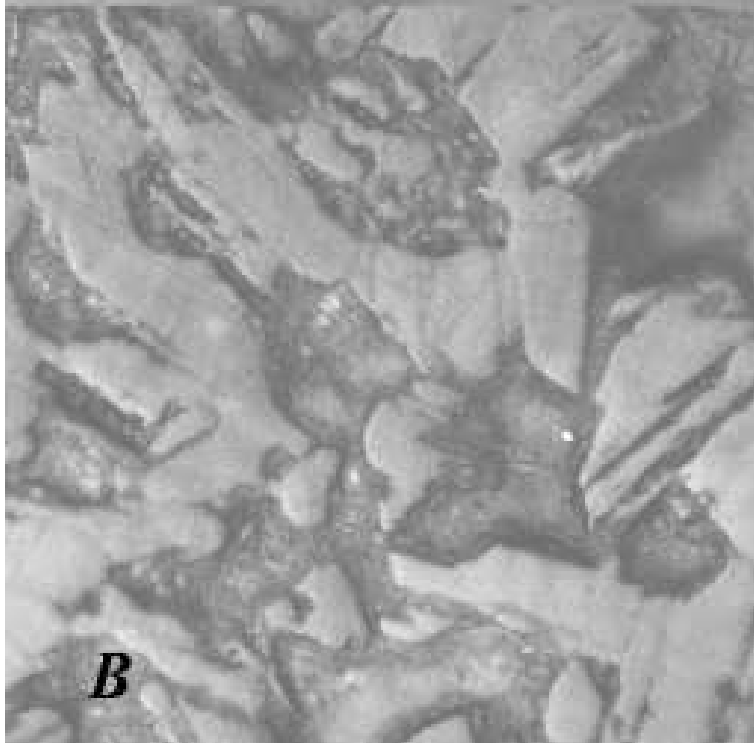
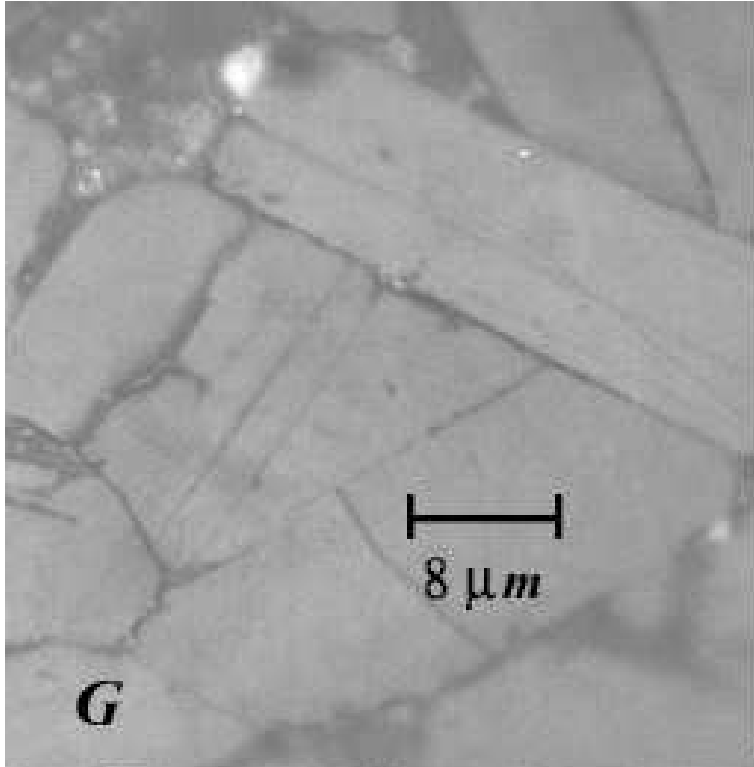
- [17] E. H. Brandt, Phys. Rev. B. **58** (1998) 6506.
- [18] P. Pereyra and A. Kunold, Phys. Rev. B **51**, 3820 (1995).
- [19] A. Kunold and P. Pereyra, Physica C **245**, 57 (1995).
- [20] P. Pereyra, J.L. Cardoso, L. E. Amezcua and A. Kunold, Physica C **266**, 81 (1996).
- [21] J.L. Cardoso and P. Pereyra, Phys. Rev. B. **61**, (2000) 6360.
- [22] Mai Suam Li, Phys. Rev. B. **60**, (1999) 118.
- [23] R.A. Hein, Phys. Rev. B **33** (1986) 7539.
- [24] A. Maeda, Y. Lino, T. Hanaguri and N. Motokina, Phys. Rev. Lett. **74** (1995)1202.

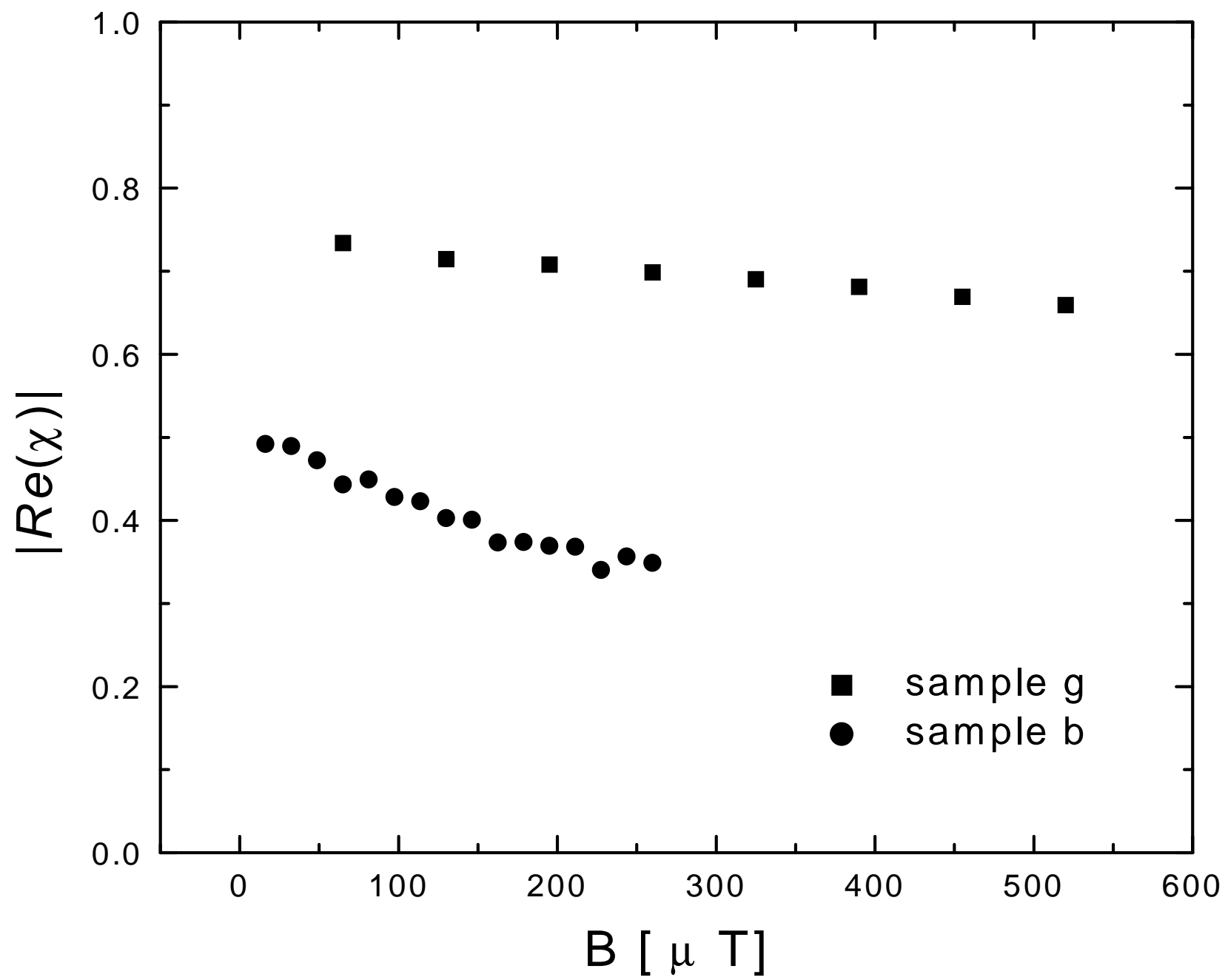
Captions

1. Microscopic images of the samples G and B.
2. The susceptibility of the good and bad samples differ in magnitude and have a qualitatively different behavior as functions of the applied magnetic field. The curves shown here are for $T = 35K$.
3. The screening currents distributions and the tunneling path in the two adjacent ceramic grains. In regions I we assume complete Meissner effect; in regions II flow the screening currents, with a density distribution as shown below, reaching a critical value at the boundary of this and regions III, where the external magnetic field penetrates; finally, the intergrain region IV is also shown.
4. An idealized picture of three adjacent grains with Josephson's junctions between them, forming an elementary tunneling circuit. Each grain has its own regions of the types I, II, and III, as explained in Figure 3. The screening currents circulate within regions II in the counter-clock direction. The intergrain tunneling current 1 circulates in the

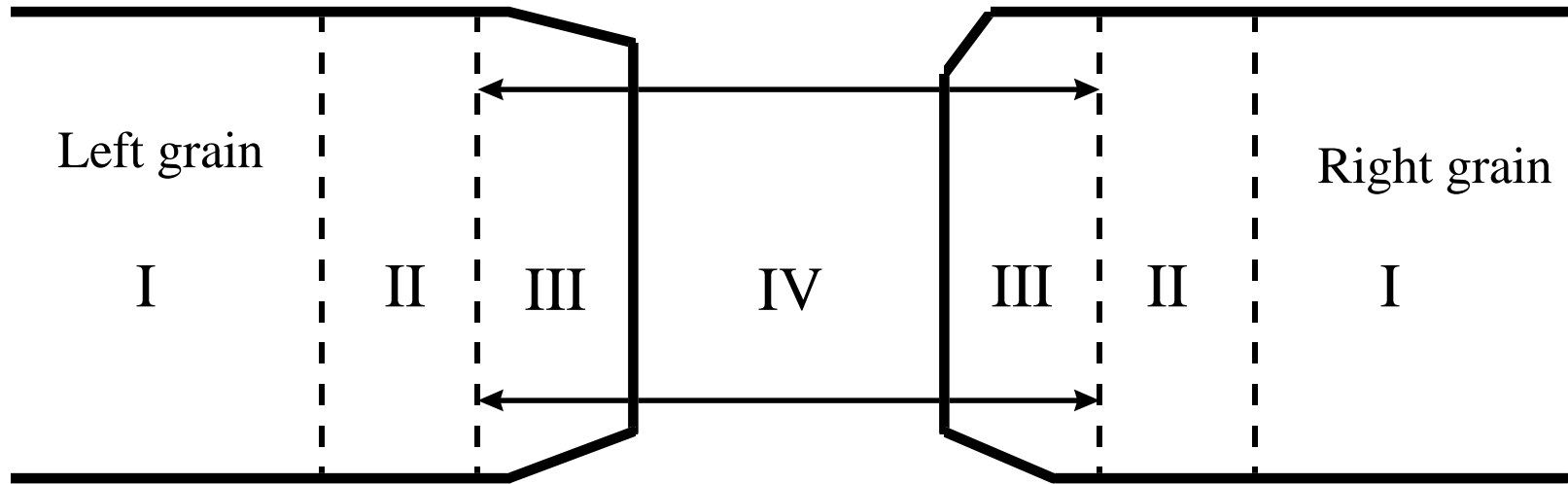
same direction in the outer part of the circuit, while the current I_2 in the inner part of the circuit has the opposite, clockwise direction. The external magnetic field can penetrate into the region III of each grain, and into the regions IV and V between the grains.

5. Behavior of χ as a function of the applied magnetic field at different temperatures for the sample B.
6. Behavior of χ as a function of the applied magnetic field at different temperatures for sample G.





Tunneling path



Current distributions

